Journal of Natural Gas Science and Engineering 88 (2021) 103853

Contents lists available at ScienceDirect

Journal of Natural Gas Science and Engineering

journal homepage: http://www.elsevier.com/locate/jngse

A novel approach to optimising well trajectory in heterogeneous reservoirs based on the fast-marching method

Zehao Lyu [a], Qinghua Lei [b,*], Liang Yang [c], Claire Heaney [d], Xianzhi Song [a], Pablo Salinas [d], Matthew Jackson [d], Gensheng Li [a], Christopher Pain [d]

[a] State Key Laboratory of Petroleum Resources and Prospecting, China University of Petroleum, Beijing, China
[b] Department of Earth Sciences, ETH Zürich, Zürich, Switzerland
[c] Division of Energy and Power, Cranfield University, Cranfield, UK
[d] Department of Earth Science and Engineering, Imperial College London, London, UK

ARTICLE INFO

Keywords:
Fast marching method
Well optimisation
Continuous-space shortest path
Heterogeneous reservoir
Productivity potential

ABSTRACT

To achieve efficient recovery of subsurface energy resources, a suitable trajectory needs to be identified for the production well. In this study, a new approach is presented for automated identification of optimum well trajectories in heterogeneous oil/gas reservoirs. The optimisation procedures are as follows. First, a productivity potential map is generated based on the site characterisation data of a reservoir (when available). Second, based on the fast-marching method, well paths are generated from a number of entrance positions to a number of exit points at opposite sides of the reservoir. The well trajectory is also locally constrained by a prescribed maximum curvature to ensure that the well trajectory is drillable. Finally, the optimum well trajectory is selected from all the candidate paths based on the calculation of a benefit-to-cost ratio. If required, a straight directional well path, may also be derived through a linear approximation to the optimised non-linear trajectory by least squares analysis. Model performance has been demonstrated in both 2D and 3D. In the 2D example, the benefit-to-cost ratio of the optimised well is much higher than that of a straight well; in the 3D example, laterals of various curvatures are generated. The applicability of the method is tested by exploring different reservoir heterogeneities and curvature constraints. This approach can be applied to determine the entrance/exit positions and the well path for subsurface energy system development, which is useful for field applications.

1. Introduction

The design of optimised well systems with their trajectories maximising the total profit while minimising the construction cost are crucial for the oil/gas industry (Lee et al., 2009). Studies have been carried out to develop optimisation techniques for such purposes in the past decades, mainly focusing on well placement optimisation (Guyaguler and Horne, 2000; Taware et al., 2012; Naderi and Khamehchi, 2017) and well trajectory optimisation (Lee et al., 2009; Xu et al., 2019; Zheng et al., 2019). Especially, the research group at Stanford University has carried out extensive studies on well placement optimisation. Badru (2003) presented an optimisation approach based on a quality map with genetic and polytope algorithms to determine optimal well locations. Onwunalu (2006) used a genetic algorithm to optimise the deployment of nonconventional wells. A proxy based on cluster analysis was applied to reduce the excessive computational requirements. Moreover, new procedures for well placement optimisation using particle swarm optimisation as the underlying algorithm have been applied to large-scale field problems (Onwunalu and Durlofsky, 2010, 2011). For some applications, particle swarm optimisation has been shown to outperform genetic algorithms (Onwunalu, 2010). Yeten et al. (2003a; 2003b) applied a genetic algorithm with an artificial neural network, a hill climber and a near wellbore upscaling, to optimise the number of producers and injectors, types, locations and trajectories. Ye (2019) applied the particle swarm optimisation method to optimise well placement with three constraints: maximum well length, minimum inter-well distance, and minimum well-to-boundary distance. The constraint-handling treatment was also found to improve optimiser performance. In addition, other methods, such as finite difference approximations (Volkov and Bellout, 2018) and mesh adaptive direct search (Isebor and Durlofsky, 2014), have also been developed. Furthermore, other researchers have used adjoint or stochastic

* Corresponding author.
E-mail addresses: qinghua.lei@erdw.ethz.ch, leiqinghua.imperial@gmail.com (Q. Lei).

https://doi.org/10.1016/j.jngse.2021.103853
Received 1 April 2020; Received in revised form 4 January 2021; Accepted 31 January 2021
Available online 7 February 2021

perturbation methods for the optimisation of well placement (Bellout and Ciaurri, 2012; Jesmani et al., 2020; Zhang et al., 2020).

For each single well, the well trajectory plays a significant role in the performance of the well and its economic viability. However, the issue of optimising well trajectories is particularly challenging. To tackle this problem, different mathematical methods have been developed, e.g. the radius-of-curvature method (Liu et al., 2004) and the minimum-curvature method (Sawaryn and Thorogood, 2005). Recently, several mathematical frameworks, such as genetic algorithms, swarm algorithms, artificial neural networks and near-well upscaling approaches, have been developed to optimise the geometrical configuration of production wells (Hamida and Azizi, 2017; Hassan et al., 2017). Other researchers have optimised sidetrack wells and horizontal wells using a heuristic differential search algorithm in conjunction with a stochastic gradient technique (Hanea and Casanova, 2017; Wang et al., 2016). Furthermore, software such as COMSOL Multiphysics have been adopted for numerical simulation to optimise multilateral wells (Chen et al., 2012).

By reviewing the literature on well trajectory optimisation, it is found that in previous studies (Atashnezhad and Wood, 2014; Mansouri et al., 2015; Wang et al., 2016), many important factors such as reservoir heterogeneities have not been adequately considered. Furthermore, the starting point and the end point of the well path are fixed in many models. The objective functional to be minimised is often based on drilling costs (related to the well length) without considering the benefits (related to the oil production potential) (Sawaryn and Tulceanu, 2009). In addition, most existing methods in the literature assumed *a priori* a regular shape for the trajectory, such as straight lines or circular arcs, before applying optimisation (Xu, 2019). This may not produce the most optimum solutions. Thus, a generalised framework is developed for optimising well trajectories in heterogeneous reservoirs in this paper. The novelty of our approach is threefold. First, reservoir heterogeneities are considered by constructing a productivity potential map based on site characterisation data. The kriging method is applied to generate a continuous geological map with appropriate and adequate grids in the 2D model. Second, instead of artificially assuming the starting and target points of the well before optimisation, as adopted in many other existing models, our method can automatically determine these points through optimisation based on the fast-marching method (FMM) (Sethian, 1996, 1999; Xie and Yang, 2012; Sharifi et al., 2014). The FMM method has been widely applied for many studies in petroleum engineering, where researchers have used it to optimise the spacing of wells or hydraulic fractures, although the trajectories are assumed to be straight paths (Al-qasim et al., 2017; Huang et al., 2017; Iino and Datta-Gupta, 2018; Paryani et al., 2018). The FMM approach has also been utilised for drainage volume research (Xie and Yang, 2012), pressure analysis (Han et al., 2018) and heat transfer calculation (Cui et al., 2016). Third, the well trajectory optimised in our method is not constrained by predetermined shapes and numbers of lines or arcs.

This paper is organised as follows. In section 2, the main theoretical principles of the fast-marching method are described. In section 3, the procedures for well trajectory optimisation based on the fast-marching method are presented. In section 4, the proposed method is applied to two-dimensional (2D) and three-dimensional (3D) heterogeneous reservoirs. Finally, a discussion and conclusions are provided in sections 5 and 6, respectively.

2. Continuous-space shortest path and fast marching method

Searching for the continuous-space shortest path is a challenging problem encountered in many research fields, e.g. robot navigation at minimum costs (Garrido and Moreno, 2011). The basic framework of such a problem is described as follows. For a starting point A and a cost function $F(x_1, x_2, \ldots, x_n)$ in a n-dimensional space R^n, the aim is to find a path $\gamma(\tau)$: $[0, \infty) \rightarrow R^n$ connecting point A to B minimising the integral (Sethian, 1999), i.e. the cumulative cost along the path, written as:

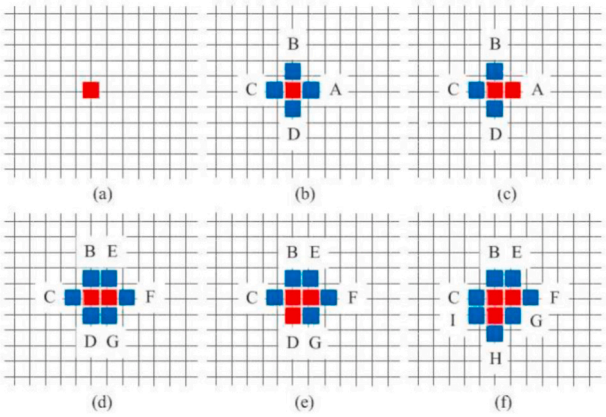

Fig. 1. A schematic showing the procedures for constructing a distance map using the fast-marching method (FMM); adapted from (Xie and Yang, 2012).

$$\int_{A=\gamma(0)}^{B=\gamma(L)} F(\gamma(\tau))d\tau \tag{1}$$

where τ is the arc-length parameterisation of γ (i.e. $|\gamma(\tau)| = 1$), and L is the total length.

For two-dimensional (2D) problems, a starting point of $A(x_0, y_0)$ and the cost function $F(x, y)$ are defined. Then, $T(x, y)$ is defined as the minimum cost to connect A to a point (x, y) (Sethian, 1999):

$$T(x,y) = \min_{\gamma} \int_{A}^{(x,y)} F(\gamma(\tau))d\tau \tag{2}$$

The function $T(x, y) = C$ represents all points in the 2D space that can be arrived at with the minimum cost C. The paths with the minimum cost are orthogonal to the level curves (T):

$$\frac{|\nabla T(x,y)|}{F(x,y)} = |\nabla T(x,y)|V(x,y) = 1 \tag{3}$$

where a speed function $V(x, y)$ is introduced as the inverse of the cost function $F(x, y)$. Here, equation (3) is an Eikonal equation and can be solved by the Fast Marching Method (FMM), which was first proposed by Sethian (1996) to calculate the propagating time at different points for fronts monotonically advancing from a starting point with different speeds. Thus, $T(x, y)$ can be seen as the arrival time at the point (x, y). $V(x, y)$ is the propagation speed (Sethian, 1999). In other words, the problem of finding the shortest path with the minimum cost can be reduced to solving the Eikonal equation, i.e. equation (3), which can be achieved by using the FMM.

To solve equation (3) using FMM, the problem domain is discretised using an orthogonal grid (Sethian, 1996, 1999). In the 2D domain, each point (x, y) has four neighbouring nodes, i.e. $(x+\Delta x, y)$, $(x-\Delta x, y)$, $(x, y+\Delta y)$ and $(x, y-\Delta y)$. Then, $T(x, y)$ can be solved from the following equations (4)–(6) with the minimum solution chosen (Sharifi and Kelkar, 2014):

$$T_1 = \min\left\{T_{(x-\Delta x,y)}, T_{(x+\Delta x,y)}\right\} \tag{4}$$

$$T_2 = \min\left\{T_{(x,y-\Delta y)}, T_{(x,y+\Delta y)}\right\} \tag{5}$$

$$|\nabla T(x,y)| = \sqrt{\left(\frac{T(x,y)-T_1}{\Delta x}\right)^2 + \left(\frac{T(x,y)-T_2}{\Delta y}\right)^2} = \frac{1}{V(x,y)} \tag{6}$$

where Δx and Δy represent the grid spacing. The solution to $T(x, y)$ in equation (3) is $T_1+1/V(x, y)$ if $T_2 > T > T_1$, $T_2+1/V(x, y)$ if $T_1 > T > T_2$, or the solution to equation (6) if $T > \max\{T_1, T_2\}$.

An example of a 5-stencil Cartesian grid is presented in Fig. 1 to

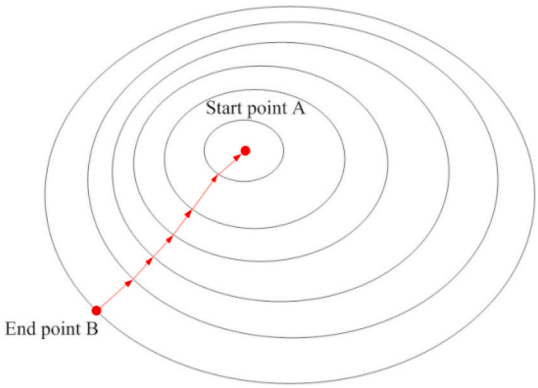

Fig. 2. Illustration of finding the shortest path from point *B* to *A* using gradient descent on a series of level sets.

illustrate the FMM algorithm, defining the middle point as the starting point (red square in Fig. 1a). The grid nodes are labelled based on three categories: unarrived nodes (whose arrival times have not been reached), occupied nodes (whose arrival times have been reached), and trial nodes (whose arrival times have been calculated but are still changeable). The basic steps are presented below:

(1) Label all nodes as "unarrived";
(2) Activate an "occupied" node (i.e. the red square in Fig. 1a) as the starting point;
(3) For the "occupied" node, mark its neighbouring "unarrived" nodes to be "trial" (markers A, B, C and D in Fig. 1b);
(4) Loop over all the nodes labelled with "trial" and calculate its arrival time from its "occupied" neighbour(s) as the minimum of local solutions to the Eikonal equation (e.g. marker A in Fig. 1c);
(5) Once the arrival time of all the nodes labelled "trial" have been predicted, the one with the minimum arrival time is recognised as a new "occupied" node (e.g. marker A in Fig. 1c);
(6) Repeat steps (3)–(5) until all points are "occupied", so that a distance map representing the minimum arrival time from the starting point is generated for the entire problem domain.

After the distance map is generated (Fig. 1), level sets radiating from a starting point *A* and covering the entire domain can be constructed (Fig. 2). For a given end point, e.g. the point *B*, identification of the shortest path is then achieved by back-propagating from *B* to *A* based on the gradient descent (Sethian, 1999):

$$X_t = \nabla T(x, y), with\ X(0) = B \tag{7}$$

Two validation examples of path planning solved using FMM are presented here. In a homogeneous 2D domain (Fig. 3a) with a constant speed function, i.e. $V(x, y)$ in equation (3), the shortest path connecting the corner points A and B is identified, i.e. the straight blue line

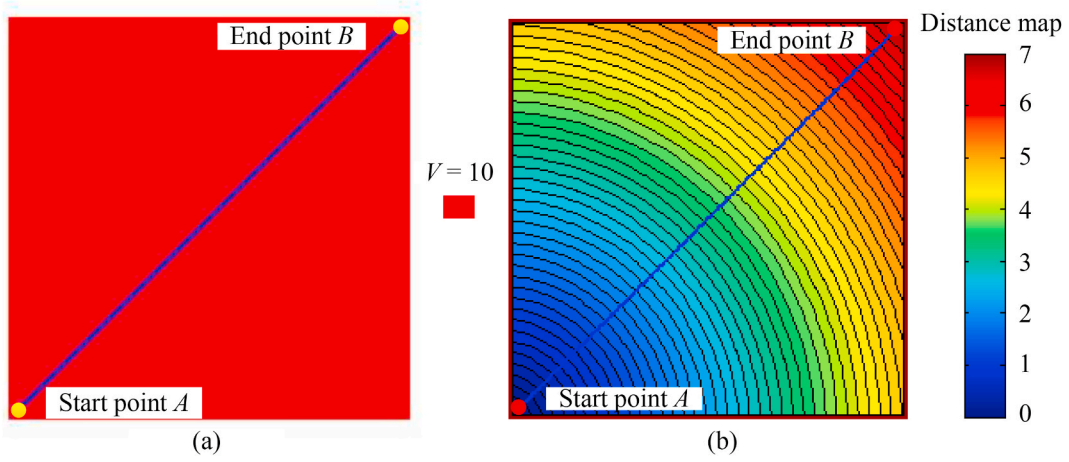

Fig. 3. The identification of the shortest path connecting the start and end points in a homogeneous domain using the fast-marching method: (a) a homogeneous field with a constant speed *V*, and (b) the corresponding distance map.

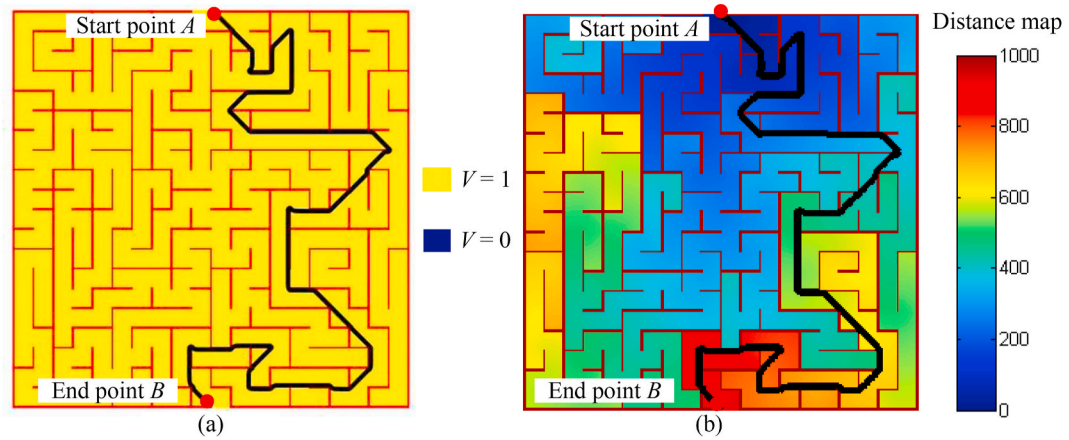

Fig. 4. Optimum path search in a maze-type heterogeneous domain using the fast-marching method: (a) the heterogeneous field involving barriers (blue) and passages (red), and (b) the corresponding distance map.

diagonally crossing the domain. It can be seen that the path follows the gradient of the distance map, which is the optimum trajectory as expected (Fig. 3b).

In Fig. 4, another demonstration example based on a maze system representing a complex heterogeneous scenario is presented. The blue barriers and red regions are associated with low and high-speed values, respectively. It can be seen that the identified shortest path (i.e. the thick black line) from point A to B avoids the barriers and passes through maze successfully, which further confirms the validity of FMM for optimum path identification.

3. Optimisation procedures of well trajectory in heterogeneous reservoirs

(1) Model assumption

The main assumptions of our optimisation approach include (i) the starting or entrance point (e.g. heel): of the well is located in a selected problem boundary, where the starting point can be randomly distributed; (ii) the well penetrates through the entire boundary and ends at the selected boundary of the exit point; (iii) the boundary pressure of the reservoir remains constant and the productivity is related to geological properties (e.g. permeability, porosity and saturation).

(2) **Mathematical modelling**

The concept of productivity potential map (equation (8)) proposed by Narayanasamy et al. (2006) is adopted to describe the heterogeneity of the reservoir. The productivity potential, P, is given as:

$$P = K\varphi S_o \tag{8}$$

where K is the permeability, φ is the porosity and S_o is the oil saturation.

(3) **Objective function**

The productivity of a well is closely associated with the well length when the productivity potential is uniformly distributed (e.g., horizontal well section). Usually, the longer the well is, the higher the productivity is, and the higher the benefit. However, longer wells also come with higher drilling costs. Thus, it is necessary to achieve a balance between the productivity and the drilling length (i.e. the highest productivity potential per well length). The benefit-to-cost ratio is calculated for all the paths associated with each particular entrance point. The objective function to be maximised is the productivity potential per well length, defined as the benefit-to-cost ratio, ζ:

$$\zeta = \frac{\int_L \phi(s)ds}{\int_L ds} \tag{9}$$

where $\phi(s)$ is the average potential value at the well intervals representing the production "benefit"; L is the total well length which is considered to be proportional to the construction "cost".

(4) **Constraints**

$$i \in \mathrm{I}\ j \in \mathrm{J} \tag{10}$$

$$|\nabla T(x,y)|P(x,y) = 1 \tag{11}$$

$$W = \nabla T(x,y), with\ W(0) = B \tag{12}$$

$$\arcsin\left(\frac{G_k c}{2000}\right) + \arcsin\left(\frac{G_{k+3} c}{2000}\right) \le q \tag{13}$$

where $i \in I$ represents an entrance point i on the assumed problem boundary I. $j \in J$ represents an exit point j on the assumed problem boundary J. $P(x, y)$ is the productivity potential. W is the generated path

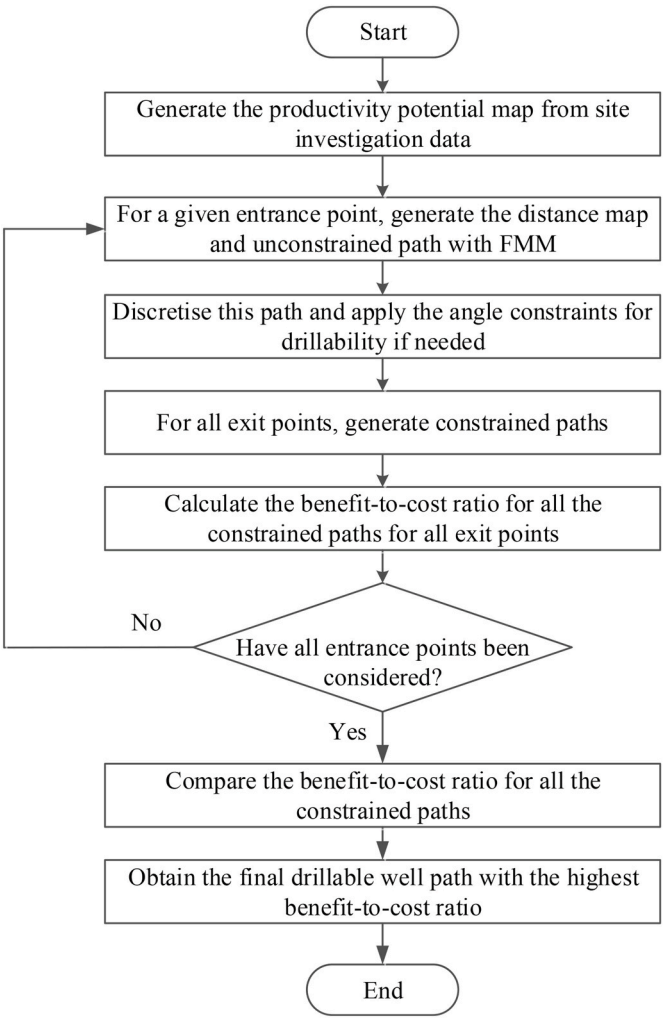

Fig. 5. Flowchart of the well trajectory optimisation method.

coordinates from one entrance point to one exit point B. Equation (11) and (12) are solved by the fast-marching method as described in section 2. In equation (13), G_k and G_{k+3} represent two adjacent constrained well sections of the discretised well path; G_{k+1} and G_{k+2}, which are between them (i.e. G_k and G_{k+3}), represent two assumed unconstrained well sections; q is the pre-determined dogleg constraint; c is the maximum local curvature.

(5) **Workflow of the algorithm**

The workflow and detailed steps for the optimisation of well trajectories is given in Fig. 5. First, pre-requisite field data (e.g. permeability, porosity and oil saturation) are collected from exploration wells. Permeability, porosity and saturation fields can be further derived by using the kriging method.

A number of entrance and exit points are selected for consideration. For a given entrance point, a corresponding distance map is constructed using the FMM based on the productivity potential map. For each exit point, an ideal unconstrained path (with no curvature constraint) is obtained using the FMM. Next, the trajectory is adjusted to avoid sharp turns according to a drilling angle constraint or dogleg constraint (Mitchell and Miska, 2011), so that the designed well path can be drillable for field application. A schematic of the dogleg constraint is given in Fig. 6, where the red curve represents the unconstrained path and the blue curve represents the constrained path obtained by imposing the dogleg constraint. The detailed procedures include:

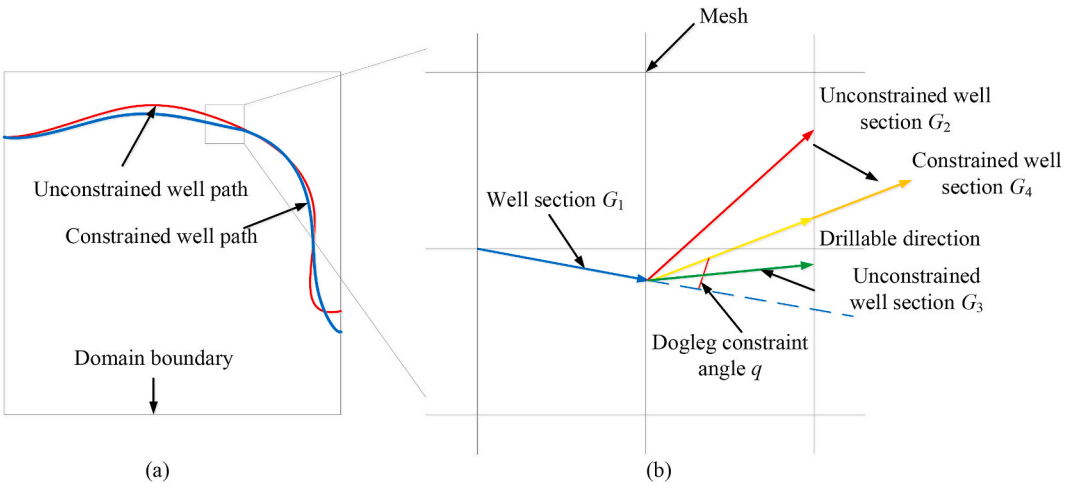

Fig. 6. (a) Comparison of the unconstrained and constrained well paths; (b) Schematic illustrating the dogleg constraint applied in the well trajectory optimisation.

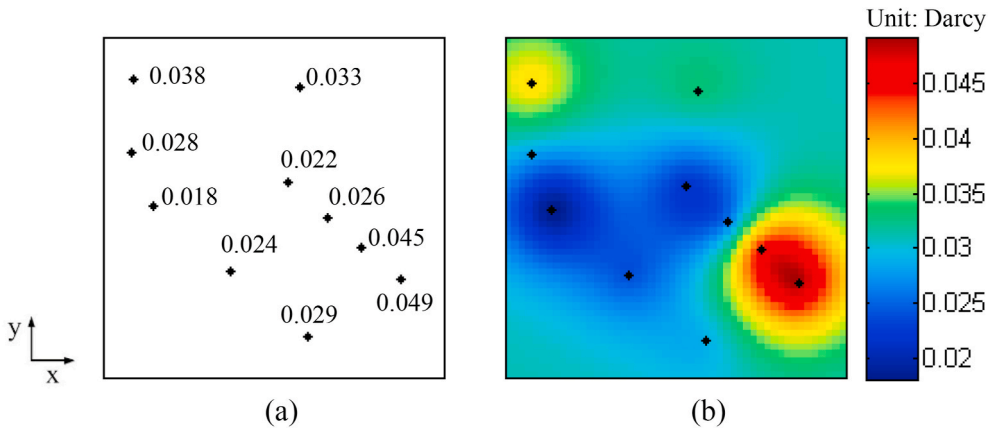

Fig. 7. (a) An oil reservoir (5 km × 5 km) characterised by a number of borehole measurements of its variable permeability field (the number is the figure indicates the local permeability measured in Darcys); (b) a constructed productivity potential map using the ordinary kriging method.

(1) Discretise the unconstrained well path using a structured mesh so that the well path can be divided into a series of sections;
(2) Focus on two adjacent well sections (e.g. well section G_1 and G_2 in Fig. 6b). The well section in the downstream grid (e.g. well section G_2) is constrained by the well direction in the upstream grid (i.e. well section G_1) due to the predefined dogleg constraint angle q. The blue dashed line is the direction of well section G_1 in the upstream grid. The angle between the possible well section direction in the downstream grid and well section G_1 needs to be less than the constraint angle. In other words, the well section in the downstream grid needs to be within the region between the blue dashed line and the yellow drillable direction, as shown in Fig. 6b. If the unconstrained well direction in the downstream grid is found to be within the drillable dogleg angle (e.g. well section G_3), the well direction will keep the same in the downstream grid. If the unconstrained well direction in the downstream grid is found to be beyond the drillable dogleg angle, the well direction will be corrected to the dogleg angle itself. For example, as shown in Fig. 6b, the red unconstrained well section G_2 is corrected to orange constrained well section G_4.
(3) Apply step (2) to the whole unconstrained well path from the given entrance point to the exit point. A constrained well path for this given entrance point can be obtained.

The procedures described above are repeated until all the entrance points have been considered. For M entrance points and N exit points, a total of $M \times N$ paths will be considered during this procedure. Finally, from all the candidate paths, the final path is selected as the one with the highest benefit-to-cost ratio, which also determines the entrance and exit points. The algorithm of the well trajectory optimisation process is also presented in the appendix.

4. Results

4.1. 2D well optimisation in heterogeneous reservoirs

Assuming a reservoir whose longitudinal dimensions are much larger than its transversal dimension, such that a horizontal well (approximately in-plane) is often drilled, a 2D model can be used to approximate the behaviour. The site characterisation data from a real reservoir (Liang, 2015) are applied to demonstrate the well optimisation method. As shown in Fig. 7a, the variable permeability field is determined based on the measurements from ten exploration boreholes distributed at different locations in a 5 km × 5 km domain. For the purposes of demonstration, the reservoir is assumed to be fully saturated by oil and the porosity is constant (e.g. 0.2). However, neither of these assumptions affect the generality of our method, which can be applied to problems where the reservoir is not fully saturated and where the porosity spatially varies. For the specific example here, permeability is the only variable affecting the productivity potential, as shown in equation (8). The domain is discretised into a 50 × 50 grid with a mesh size of 100 m. A coordinate system is defined with its origin at the left bottom corner of

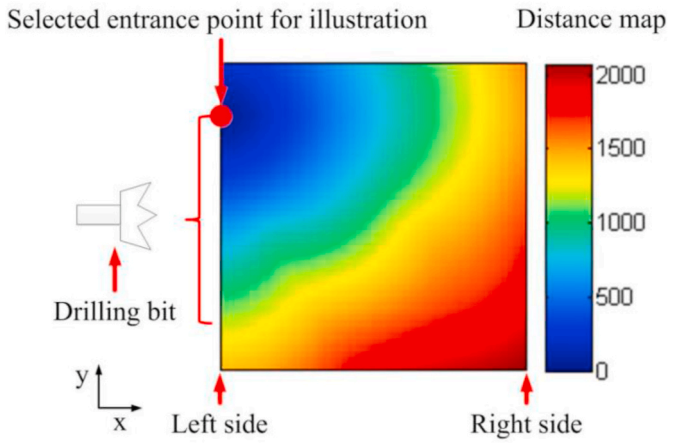

Fig. 8. The distance map for a selected entrance point as the starting position of the well path in the problem domain (5 km × 5 km).

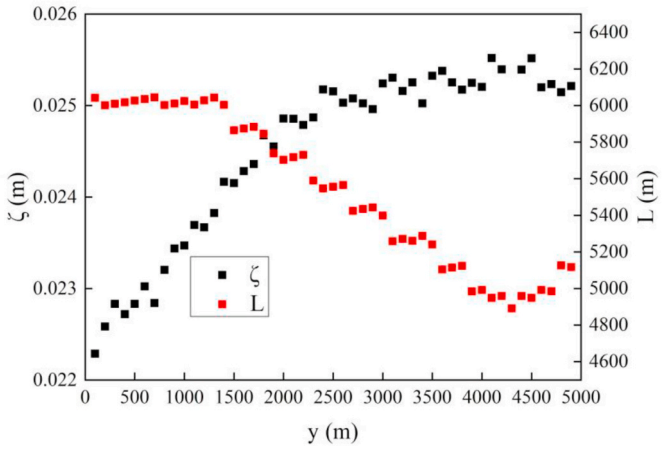

Fig. 9. Benefit-to-cost ratio, ζ, and optimised well length, L, of different exit points (coordinate y).

the domain (Fig. 7a). A productivity potential field (Fig. 7b) is then derived by interpolating/extrapolating from the measurement locations using the ordinary kriging method (Chabala and Mulolwa, 2017; Hu and Shu, 2015; Jang et al., 2016). We use an implementation of the kriging method by Schwanghart (2010).

The starting point or entrance point (e.g. heel) of the well is located along the left boundary of the problem domain. The well penetrates through the entire domain and ends at the right boundary (the exit point). Thus, a horizontal well is to be drilled across the domain starting from an entrance point located at the left boundary. A number of candidate entrance points are looped over at the left boundary, located at intervals of 200 m in the y coordinate. To avoid boundary effects, the y coordinate of the entrance point is restricted to be within the range of 1000–4000 m (see Fig. 8). There is no restriction on the y coordinate of the exit points which are considered in the range of 100–4900 m with an interval of 100 m. This will result in 784 constrained paths in total.

For clarification of the procedure, the analysis is based on one of the candidate entrance points, which will then be repeated for the remaining entrance points. A distance map for the problem domain is first constructed for a given entrance point (Fig. 8). Then, all the possible exit points are looped over at the right boundary, and for each exit point, FMM is used to generate a path penetrating the domain through regions of high productivity potential as much as possible. In this study, we use Kroon's implementation of the FMM (Kroon, 2011). In the algorithm presented in this paper, to ensure the drillability of the well, a threshold

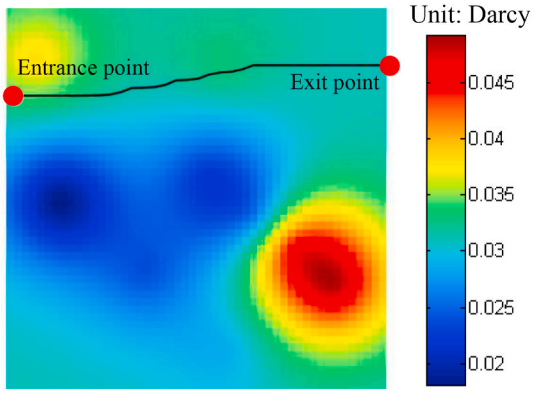

Fig. 10. The final optimum, curvature-constrained well trajectory for the heterogeneous reservoir.

value of the dogleg constraint is defined to obtain a set of drillable well paths for each exit point. The procedure is carried out for the remaining entrance points. Finally, by comparing the benefit-to-cost ratios of all the constrained paths, an optimum drilling path is identified for the well. To better elaborate the comparison process, the case where the entrance point is at a y-coordinate of 4000 m of the left boundary is taken as an example. Fig. 9 shows the benefit-to-cost ratios and optimised well lengths of different exit points of the right boundary for the entrance point mentioned above. The dogleg constraint is defined to be 30°. For this particular entrance point, the highest benefit-to-cost ratio is the optimised exit point when the well entrance point is at a coordinate of 4000 m on the left side of the domain. Considering all entrance points, the final constrained optimised well trajectory can be seen in Fig. 10 and has a total length of 5055 m, a minimum radius of curvature of 227 m, an entrance height of 3800 m and an exit point at 4200 m. The benefit-to-cost ratio of the optimised well is 0.0284, which is much higher than the ratio (i.e. 0.0031) of the straight well in Fig. 11.

The final path does not pass through the region with a high productivity potential. In order to do so, the path would first have to pass through a region of low productivity potential, and the algorithm determines that a better benefit-to-cost ratio is obtained by drilling through regions of medium productivity potential.

Here, the effects of the dogleg constraint angle on the optimisation results of well trajectories are also explored. The c in Fig. 11 represents the maximum curvature of the optimum well path after being generated. It can be seen that the optimised path gradually becomes a straight line as the dogleg angle constraint is decreased (i.e. the permitted amount of angular deviation from a straight line is reduced). Considering the technical limitations in drilling engineering, the constraint angle (as illustrated in Fig. 6) needs to be adjustable for this method to be of practical use. For field applications, it might be easier to drill a well with a small curvature. However, it may miss some regions of high productivity potential (i.e. red areas in Fig. 11).

Different productivity potential fields are also tested, which are randomly generated for the purposes of demonstration (Fig. 12). Cases 1 to 3 correspond to the permeability fields associated with the productivity potentials, and the final well trajectories as determined by the method described. The entrance points for cases 1 to 3 are 2000 m, 3600 m and 3800 m respectively. It can be seen that the proposed optimisation method can identify an optimum path that effectively passes through regions of high productivity potential in different testing cases of complex heterogeneity conditions.

4.2. 3D well optimisation in heterogeneous reservoirs

In this 3D example, a synthetic heterogeneous reservoir model is constructed for demonstration purposes, although the method described in this study is applicable to real problems if field data is available,

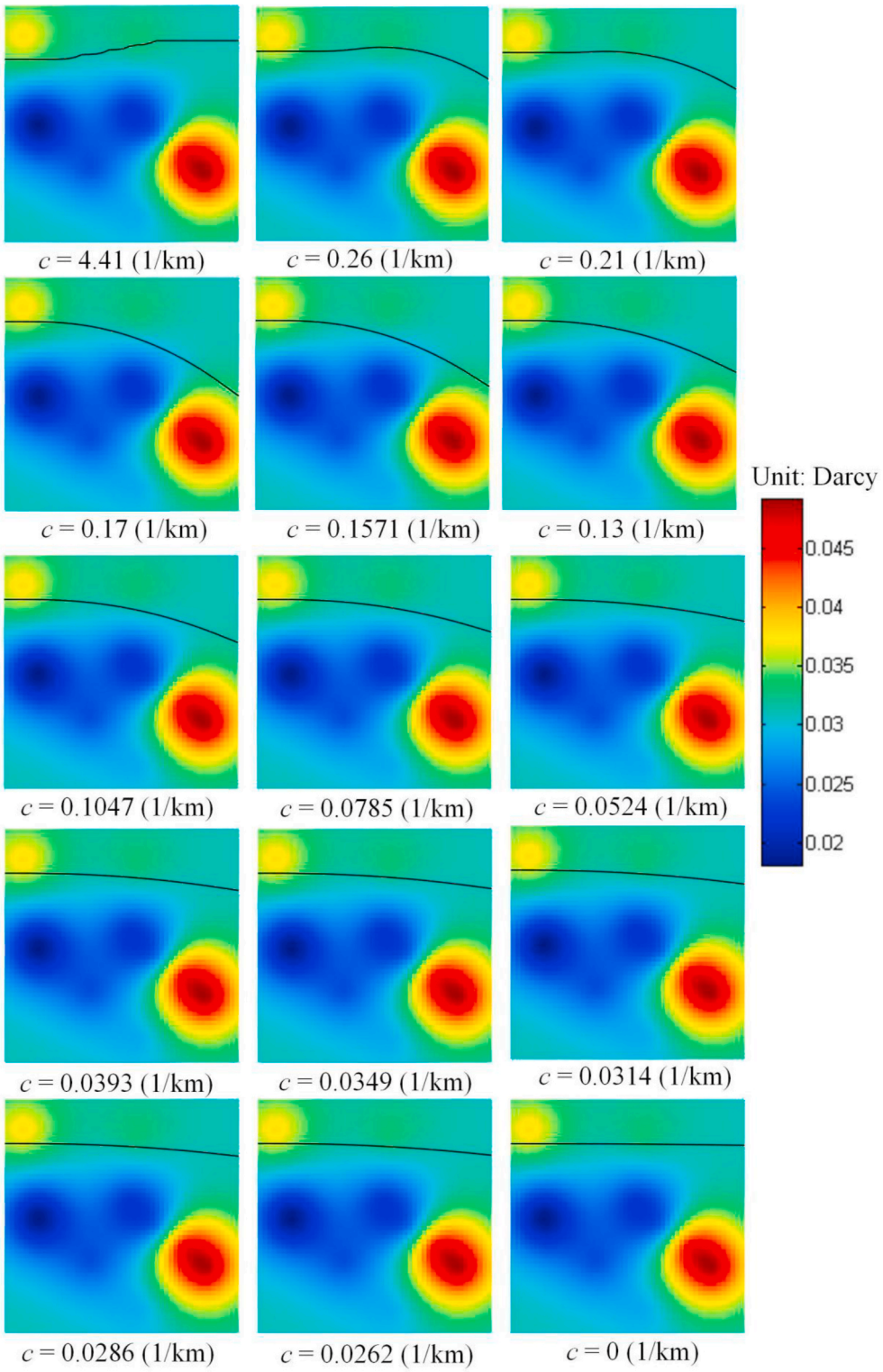

Fig. 11. Optimised well trajectories in the heterogeneous reservoir subject to different curvature constraints. Here, c denotes the maximum curvature of the well path.

which has been demonstrated in the last section, where the kriging method was applied to field data to reconstruct the permeability field. The approach can be equally applied to both field and synthetic data, in both 2D and 3D.

The problem domain in the 3D case is assumed to be a cuboid, and five potential entrance points are located on the upper side with coordinates given as (25, 25), (5, 5), (5, 45), (45, 5), (45, 45) (Fig. 13). Porosity and saturation are assumed to be constant throughout the heterogeneous reservoir. A 3D random permeability field (i.e. productivity potential), is generated based on the principles of spatial frequency and elementary waves. In order to introduce spatial variation, trigonometric functions are used in the form of $\cos(\vec{\alpha}\cdot\vec{x})$, where $\vec{\alpha} = 2\pi(k,l,m)$ is the wavevector, $|\vec{\alpha}|$ is the wavenumber and $\vec{x} = (x,y,z)$. Here, k, l and m are integers. Then the permeability (i.e. productivity

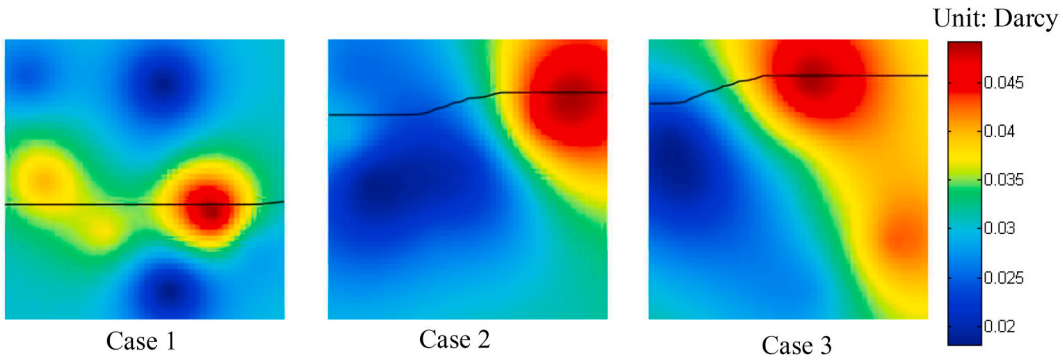

Fig. 12. Optimised well trajectories in heterogeneous reservoirs with different productivity potential distributions.

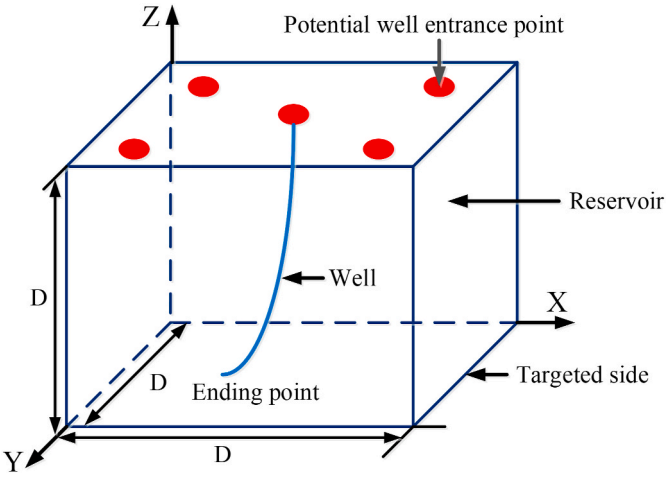

Fig. 13. Schematic of the 3D well trajectory optimisation problem.

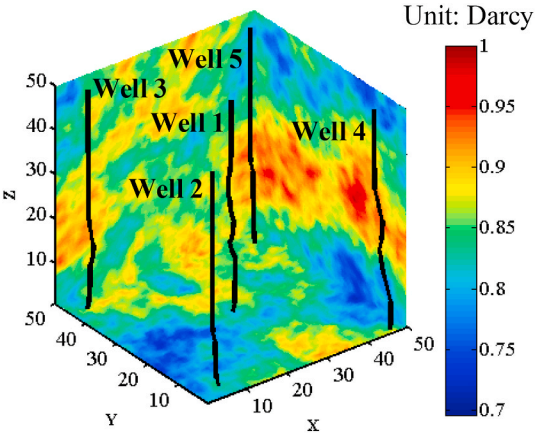

Fig. 15. Optimised well paths for five entrance points.

Table 1
Specific values of the parameters for synthetic random field generation.

Parameter	Value
K, L, M	20
Mean of the Gaussian distribution	0.8553
Standard deviation of the Gaussian distribution	1
Mean of the uniform distribution	0
Range of the uniform distribution	$-\pi/2$, $\pi/2$
β	1.8

potential) field of a heterogeneous reservoir can be described as the sum of several elementary waves given by

$$f(x,y,z) = \sum_{k=-K}^{K}\sum_{l=-L}^{L}\sum_{m=-M}^{M} A(k,l,m)\cos(\vec{\alpha}\cdot\vec{x}+\phi) \tag{14}$$

where $\phi(k, l, m)$ represents the phase angle of a uniform random distribution in the range of $-\pi/2$ and $\pi/2$, due to the assumption of an equal probability. In the natural system, larger amplitudes are more frequent with small oscillations. To generate a realistic system, the amplitude $A(k, l, m)$ is given as

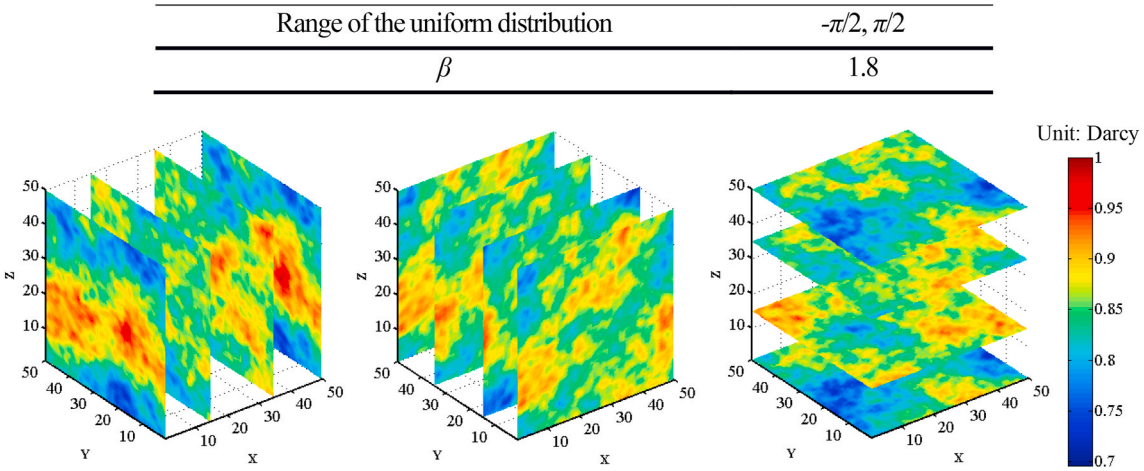

Fig. 14. Productivity potential of the 3D synthetic reservoir.

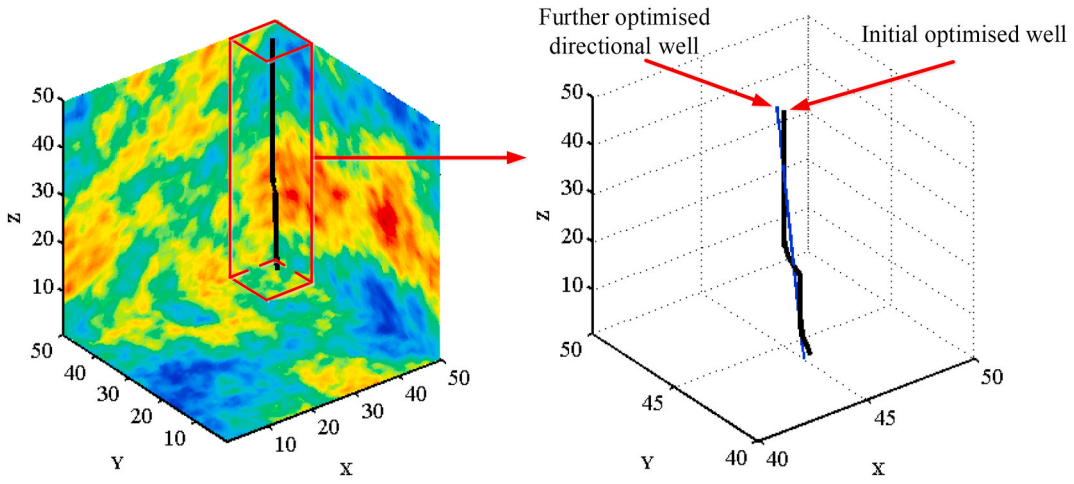

Fig. 16. Schematic of optimised well and further optimised straight well using the least squares method.

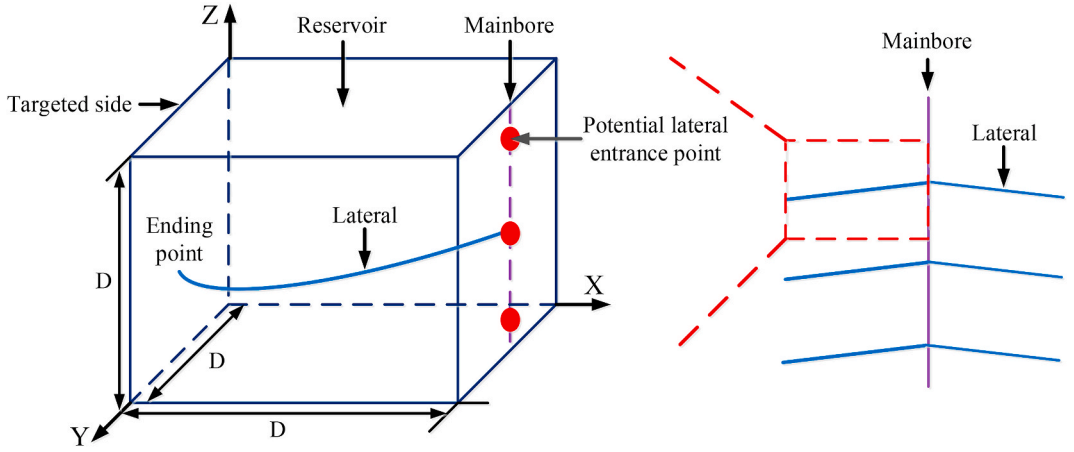

Fig. 17. Schematic of the 3D lateral trajectory optimisation problem in a multilateral well.

$$A(k,l,m) = g\left(k,l,m\right)h\left(k,l,m\right) = \frac{g(k,l,m)}{\left|k^2+l^2+m^2\right|^{\beta}} = \frac{g(k,l,m)}{\left(k^2+l^2+m^2\right)^{\beta/2}} \tag{15}$$

where $g(k, l, m)$ represents a random Gaussian distribution, $h(k, l, m)$ is a function with frequency-dependent amplitude tapering off in the range of higher wavenumbers in conformity with the spectral exponent β (where $\beta > 0$).

Table 1 gives the specific values for the different statistical parameters in our model. The domain is discretised into a 50 × 50 × 50 grid system and the width of the domain is 5 km. Fig. 14 gives the simulated distribution of productivity potential for the 3D synthetic heterogeneous reservoir models.

The optimised well paths for five different entrance points are shown in Fig. 15. In addition, as shown in Fig. 16, a straight well can be further generated by applying the least squares fitting method based on the mathematically optimum well path.

Furthermore, the proposed method can also be applied to optimise trajectories of horizontal wells or laterals as part of multilateral wells. Fig. 17 shows one lateral starting from the mainbore to the targeted side (left side in the figure) in a multilateral well. Here, three potential entrance points are analysed for illustration purposes, but more entrance points may be analysed if required.

As shown in Fig. 18, three paths may be considered as three laterals to be drilled if their spacing corresponds to the design value. Alternatively, one final optimised lateral can be further obtained through comparing benefit-to-cost ratio of the paths. In Fig. 19, optimised laterals can be slightly different due to various limitations on radii of curvature. Compared with vertical wells, drilling a lateral through the mainbore with strong local curvature can be more difficult. Thus, straight paths for laterals can also be derived with a least squares analysis.

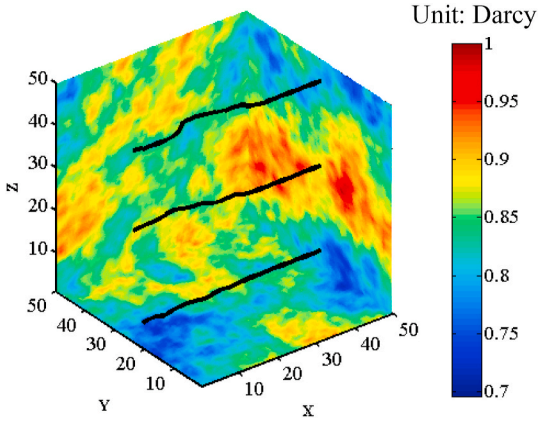

Fig. 18. Optimised horizontal laterals starting from various entrance points along the mainbore.

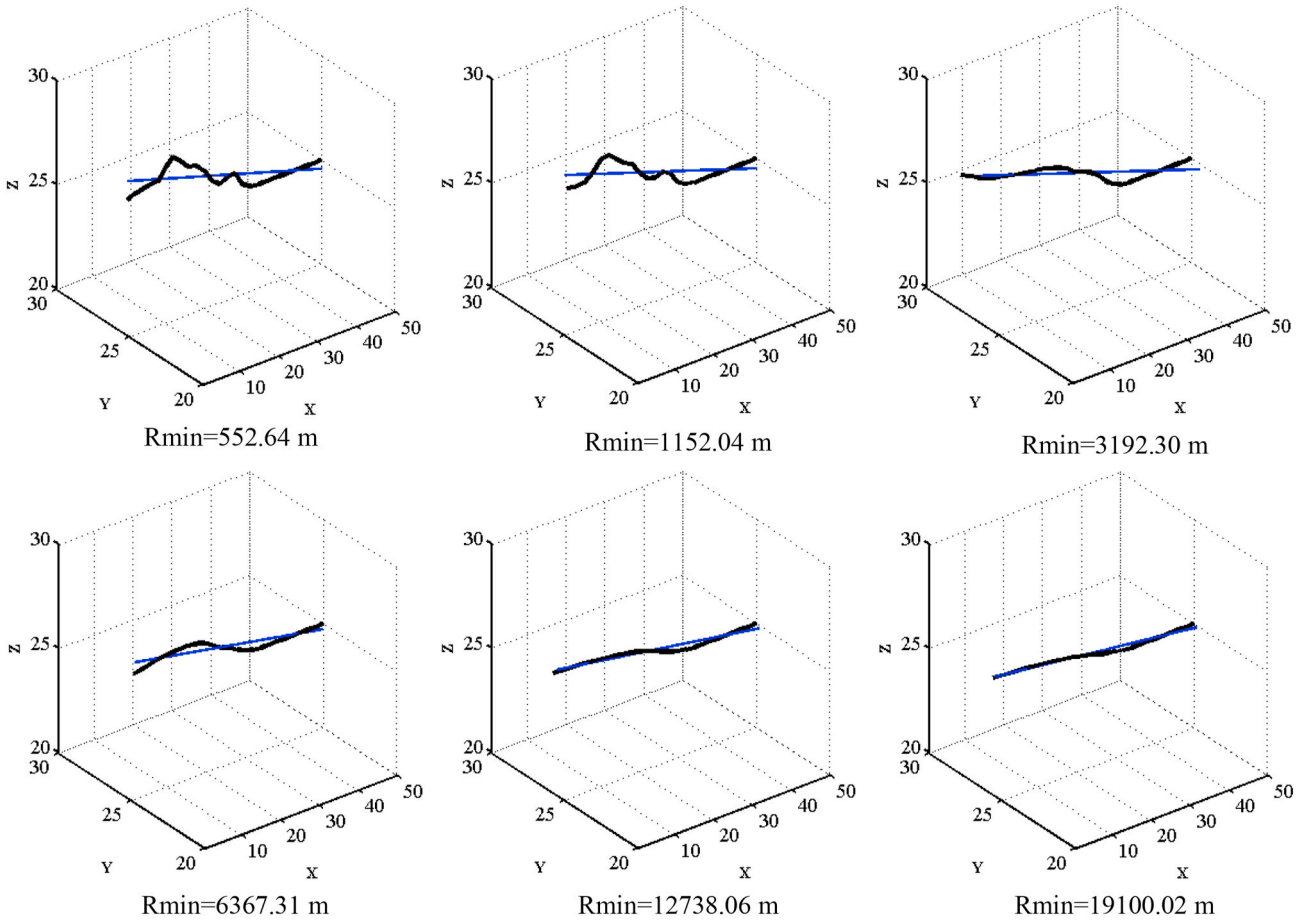

Fig. 19. Optimised horizontal laterals associated with various radii of curvature.

5. Discussion

The concept of using a productivity potential map (e.g. permeability field) to optimise well trajectories has been adopted by many researchers due to its simplicity and intuitiveness (Kharghoria and Cakici, 2003; Taware, 2012). Most have used it to identify "important" regions with good geological properties (e.g. high permeability) in the field, such that vertical or horizontal wells can be optimally placed for enhanced production (Filho, 2005; Ravalec, 2012). In this paper, a productivity potential map is used based on the permeability, porosity and saturation data as the reference for optimising the well drilling path. For the well trajectory optimisation problem in this study, the well path is generated by replacing the speed function $V(x, y)$ in equation (3) with the productivity potential of equation (8). The FMM is employed for the purpose of well optimisation, which may represent a first attempt at applying the FMM approach to optimise the well trajectory of a non-straight and curvature-constrained path. Compared with other well trajectory optimisation methods (Liu et al., 2004; Sawaryn et al., 2005, 2009; Atashnezhad et al., 2014; Mansouri et al., 2015; Wang et al., 2016; Xu et al., 2019), the presence of geological heterogeneities can be considered and their influences are modelled quantitatively via the productivity potential map. The entrance and exit points can be optimised and selected by comparing the benefit-to-cost ratios of various well trajectories in the optimisation process. Moreover, the well trajectory optimised in our method does not rely on any assumption of the path shapes and geometries. In addition, the model proposed in this paper aims to provide fast solutions to the complex optimisation problem of well trajectories in heterogeneous reservoirs (the simulation time can be as little as a few minutes on standard desktop computers). It is worth mentioning that in this paper the benefit-to-cost ratio is used to evaluate the economic viability, which is slightly different from some previous researchers who used the Net Present Value (NPV) as an objective functional (Badru, 2003; Onwunalu, 2006; Ye, 2019). However, similar results are expected to be produced by the two metrics. Our method is also easy to use and convenient for the field application due to the short time it takes for optimisation. In this paper, orthogonal grid is applied for demonstration, whereas the use of non-orthogonal grids may be explored in the future.

6. Conclusions

In this paper, a new optimisation workflow based on the fast marching method is developed and applied for optimising well trajectories in heterogeneous oil/gas reservoirs. We have elaborated the detailed procedures of this optimisation algorithm, which searches for the optimum path by maximising the benefit-to-cost ratio. The model has been validated based on a homogeneous reservoir scenario and a heterogeneous maze system. To enable the applicability of this model for oil/gas field drilling problems, we have implemented a dog-leg constraint algorithm to take into account the curvature requirement of well paths and ensure their drillability according to a prescribed threshold. The capability and performance of this well optimisation approach have been demonstrated in a series of 2D and 3D simulation studies, where single well trajectory is optimally predicted and multiple laterals of various curvatures are optimally designed. Our research findings have important implications for a broad range of geo-engineering problems involving well design and construction, such as hydrocarbon resource extraction, geothermal energy production and carbon dioxide sequestration as well as waste water reinjection.

Author statement

Zehao Lyu: Methodology, Validation, Formal analysis, Investigation, Writing - Original Draft. **Qinghua Lei:** Conceptualization, Methodology, Investigation, Writing - Review & Editing, Supervision. **Liang Yang:** Conceptualization, Methodology, Software, Writing - Review & Editing, Supervision. **Claire Heaney:** Writing - Review & Editing, Supervision. **Xianzhi Song:** Project administration, Supervision. **Pablo Salinas:** Methodology, Supervision. **Matthew Jackson:** Project administration, Funding acquisition. **Gensheng Li:** Project administration, Funding acquisition, Supervision. **Christopher Pain:** Project administration, Funding acquisition, Supervision, Writing - Review & Editing.

Declaration of competing interest

The authors declare that they have no known competing financial interests or personal relationships that could have appeared to influence the work reported in this paper.

Acknowledgements

The authors would like to acknowledge the China Petroleum Engineering Design Competition for providing the field data for this study. The authors also thank support from the China-UK joint project of Smart GeoWells (grant numbers: 2016YFE0124600 and EP/R005761/1). The first author is also grateful for the support from the China Scholarship Council (grant number: 201706440064). The source code of the well optimisation model developed in this paper is publicly accessible at the MATLAB Central File Exchange (https://ww2.mathworks.cn/matlabcentral/fileexchange/85163-well-optimisation). The code also calls the open source code of kriging method by Wolfgang Schwanghart and that of fast marching method by Dirk-Jan Kroon, the links of which can be found in the reference list of this paper.

Appendix

Algorithm: well trajectory optimisation.

(1) Initialise the geological condition (permeability, porosity and saturation) using equation (8)
(2) If the geological data are scattered points, apply the kriging method to generate a continuous productivity potential map as shown in Fig. 7
(3) Define the dogleg constraint angle $\boldsymbol{q}$, number of grids at each direction $\boldsymbol{K}$, candidate entrance points $\boldsymbol{I}$ (e.g. the left boundary in Fig. 8), and candidate exit points $\boldsymbol{J}$ (e.g. the right boundary in Fig. 8)
(4) For $\boldsymbol{i} = 1$: $\boldsymbol{I}$
(5) Generate the ith distance map based on the FMM based on equations (3)–(6) as shown in Fig. 8
(6) **For** $\boldsymbol{j} = 1$: $\boldsymbol{J}$
(7) Generate the unconstrained well path using the FMM for $\boldsymbol{i}$th entrance point and $\boldsymbol{j}$th exit point
(8) Discretise the unconstrained well path into $\boldsymbol{K}$ sections
(9) **For** $\boldsymbol{k} = 1$: $\boldsymbol{K}$
(10) Calculate the angle between section $\boldsymbol{k}$ and section $\boldsymbol{k}$+1, as shown in Fig. 6
(11) **If** angle $< \boldsymbol{q}$, **Continue; End**
(12) **If** angle $> \boldsymbol{q}$, Correct the well section $\boldsymbol{k}$+1 to the closest drillable direction; **End**
(13) Calculate and store the benefit-to-cost ratios of each well path and well path coordinates
(14) **End**
(15) **End**
(16) End
(17) Compare the benefit-to-cost ratios
(18) Select the well path with the highest benefit-to-cost ratio (e.g. Fig. 10)

References

Al-qasim, A., Aramco, S., 2017. Optimizing well locations in green fields using fast marching method : optimize well locations without upscaling using hundreds of scenarios and realizations with high accuracy in minutes overview of FMM. In: SPE Western Regional Meeting Held in Bakersfield. California, USA.
Atashnezhad, A., Wood, D.A., 2014. Designing and optimizing deviated wellbore trajectories using novel particle swarm algorithms. J. Nat. Gas Sci. Eng. 21, 1184–1204.
Badru, O., 2003. Well-placement Optimization Using the Quality Map Approach. Master thesis. Stanford University.
Bellout, M.C., Ciaurri, D., 2012. Joint optimization of oil well placement and controls. Comput. Geosci. 16, 1061–1079.
Chabala, L.M., Mulolwa, A., 2017. Application of ordinary kriging in mapping soil organic carbon in Zambia. Pedosphere 27 (2), 338–343.
Chen, D., Pan, Z., 2012. Characteristic of anisotropic coal permeability and its impact on optimal design of multilateral well for coalbed methane production. J. Petrol. Sci. Eng. 88–89, 13–28.
Cui, J., Yang, C., 2016. Diagnosis in multiple-stage-stimulated horizontal well by temperature measurements with fast marching method. SPE J. 21 (06), 2289–2300.
Filho, J.S.D.A.C., 2005. Methodology for Quality Map Generation to Assist with the Selection and Refinement of Production Strategies. SPE Annual Technical Conference and Exhibition, Dallas, Texas, USA.
Garrido, S., Moreno, L., 2011. Path planning for mobile robot navigation using voronoi diagram and fast marching. In: IEEE/RSJ International Conference on Intelligent Robots and Systems. Beijing, China.
Guyaguler, B., Horne, R.N., 2000. Optimization of Well Placement in a Gulf of Mexico Waterflooding Project. SPE Annual Technical Conference and Exhibition, Dallas, Texas, USA.
Hamida, Z., Azizi, F., 2017. An efficient geometry-based optimization approach for well placement in oil fields. J. Petrol. Sci. Eng. 149, 383–392.
Han, J., Yang, C., 2018. Transient pressure analysis of horizontal well with nonorthogonal transverse fractures and drainage volume characterization using fast marching method. Journal of Natural Gas and Engineering 54, 110–119.
Hanea, R.G., Casanova, P., 2017. Well trajectory optimization constrained to structural uncertainties. In: SPE Reservoir Simulation Conference. Montgomery, TX, USA.
Hassan, A., Abdulraheem, A., 2017. New approach to quantify productivity of fishbone multilateral well. In: SPE Annual Technial Conference and Exhibition. San Antonio, Texas, USA.
Hu, H., Shu, H., 2015. An improved coarse-grained parallel algorithm for computational acceleration of ordinary Kriging interpolation. Comput. Geosci. 78, 44–52.
Huang, J., Olalotiti-lawal, F., 2017. Modeling Well Interference and Optimal Well Spacing in Unconventional Reservoirs Using the Fast Marching Method. SPE/AAPG/SEG Unconventional Resources Technology Conference, Austin, Texas, USA.
Iino, A., Datta-Gupta, A., 2018. Optimizing CO_2 and field gas injection EOR in unconventional reservoirs using the fast marching method. In: SPE Improved Oil Recovery Conference. Tulsa, Oklahoma, USA.
Isebor, O.J., Durlofsky, L.J., 2014. A derivative-free methodology with local and global search for the constrained joint optimization of well locations and controls. Comput. Geosci. 18, 463–482.
Jang, C., Chen, S., 2016. Spatial estimation of the thickness of low permeability topsoil materials by using a combined ordinary-indicator kriging approach with multiple thresholds. Eng. Geol. 207, 56–65.
Jesmani, M., Jafarpour, B., 2020. A reduced random sampling strategy for fast robust well placement optimization. J. Petrol. Sci. Eng. 184, 106414.

Kharghoria, A., Cakici, M., 2003. Productivity-based method for selection of reservoir drilling target and steering strategy. In: SPE/IADC Middle East Drilling Technology Conference and Exhibition. UAE, Abu Dhabi.
Kroon, D.-J., 2011. Accurate fast marching (MATLAB Central File Exchange). https://www.mathworks.com/matlabcentral/fileexchange/24531-accurate-fast-marching.
Lee, J.W., Park, C., 2009. Horizontal well design incorporated with interwell interference, drilling location, and trajectory for the recovery optimization. In: SPE/EAGE Reservoir Characterization and Simulation Conference. Abu Dhabi, UAE.
Liang, Y., 2015. Guide for the China Petroleum Engineering Design Competition.
Liu, X.S., Liu, R.S., 2004. New techniques improve well planning and survey calculation for rotary-steerable drilling. In: IADC/SPE Asia Pacific Drilling Technology Conference and Exhibition. Kuala Lumpur, Malaysia.
Mansouri, V., Khosravanian, R., 2015. 3-D well path design using a multi objective genetic algorithm. J. Petrol. Sci. Eng. 27, 219–235.
Mitchell, R., Miska, S., 2011. FUNDAMENTALS OF DRILLING ENGINEERING.
Naderi, M., Khamehchi, E., 2017. Well placement optimization using metaheuristic bat algorithm. J. Petrol. Sci. Eng. 150, 348–354.
Narayanasamy, R., Davies, D.R., 2006. Well location selection from a static model and multiple realisations of a geomodel using productivity - potential map technique. SPE Europec/EAGE Annual Conference and Exhibition, Vienna, Austria.
Onwunalu, J., 2006. Optimization of Nonconventional Well Placement Using Genetic Algorithms and Statistical Proxy. Master thesis. Stanford University.
Onwunalu, J., 2010. Optimization of Field Development Using Particle Swarm Optimization and New Well Pattern Descriptions. Ph.D thesis. Stanford University.
Onwunalu, J., Durlofsky, L.J., 2010. Application of a particle swarm optimization algorithm for determining optimum well location and type. Comput. Geosci. 14, 183–198.
Onwunalu, J., Durlofsky, L.J., 2011. A new well-pattern-optimization procedure for large-scale field development. SPE J. 594–607.
Paryani, M., Bachir, A., 2018. Engineered Completion and Well Spacing Optimization Using a Geologically and Geomechanically Constrained 3D Planar Frac Simulator and Fast Marching Method: Application to Eagle Ford. SPE Western Regional Meeting, Garden Grove, California, USA.
Ravalec, M.L., 2012. Optimizing well placement with quality maps derived from multi-fidelity meta-models. In: EAGE Annual Conference and Exhibition Incorporating SPE Europec. Copenhagen, Denmark.
Sawaryn, S.J., Thorogood, J.L., 2005. A compendium of directional calculations based on the minimum-curvature method. SPE Drill. Complet. 24–36.
Sawaryn, S.J., Tulceanu, M.A., 2009. A compendium of directional calculations based on the minimum-curvature method-part 2: extension to steering and landing applications. SPE Drill. Complet. 311–325.
Schwanghart, W., 2010. Ordinary kriging (MATLAB Central File Exchange). https://www.mathworks.com/matlabcentral/fileexchange/29025-ordinary-kriging.
Sethian, J.A., 1996. A fast marching level set method for monotonically advancing fronts. Proc. Natl. Acad. Sci. Unit. States Am. 93, 1591–1595.
Sethian, J.A., 1999. Fast marching methods. SIAM Rev. 41, 199–235.
Sharifi, M., Kelkar, M., 2014. Novel permeability upscaling method using fast marching method. Fuel 117, 568–578.
Taware, S., Park, H., 2012. Well placement optimization in a mature carbonate waterflood using streamline-based quality map. In: SPE Oil and Gas India Conference and Exhibition. Mumbai, India.
Volkov, O., Bellout, M., 2018. Gradient-based constrained well placement optimization. J. Petrol. Sci. Eng. 171, 1052–1066.
Wang, Z., Gao, D., 2016. Multi-objective side-tracking horizontal well trajectory optimization in cluster wells based on DS algorithm. J. Petrol. Sci. Eng. 147, 771–778.
Xie, J., Yang, C., 2012. Integration of Shale Gas Production Data and Microseismic for Fracture and Reservoir Properties Using Fast Marching Method. SPE Eastern Regional Meeting. Kentucky, USA.
Xu, Y., 2019. Research on well trajectory optimization design based on ant colony algorithm. J. Phys. Conf. 1237, 022056.
Ye, T., 2019. Treatment of Geometric Constraints in Well Placement Optimization. Master thesis. Stanford University.
Yeten, B., 2003. Optimum Deployment of Nonconventional Wells. Ph.D thesis. Stanford University.
Yeten, B., Durlofsky, L.J., 2003. Optimization of nonconventional well type, location, and trajectory. SPE J. 8, 200–210.
Zhang, J., Feng, Q., 2020. A two-stage step-wise framework for fast optimization of well placement in coalbed methane reservoirs. Int. J. Coal Geol. 225, 103479.
Zheng, J., Lu, C., 2019. Multi-objective cellular particle swarm optimization for wellbore trajectory design. Appl. Soft Comput. 77, 106–117.